DOI: 10.13009/EUCASS2023-560
Aerospace Europe Conference 2023 – 10TH EUCASS – 9TH CEAS

# Quick-preliminary aerodynamic estimation for a distributed propulsion aircraft with propellers in front of the wing

David Planas*
*ISAE-Supaero, DCAS, Toulouse, France, 31400*
*ONERA, DTIS, Toulouse, France, 31400*

Eric Nguyen Van†
*ONERA, DTIS, Toulouse, France, 31400*

Carsten Döll‡
*ONERA, DTIS, Toulouse, France, 31400.*

Philippe Pastor§
*ISAE-Supaero, DCAS, Toulouse, France, 31400*

**The following paper presents the development and validation of a modeling for the quick estimation of the aerodynamic forces and moments of a distributed electric propulsion aircraft (DEP). The use of DEP concepts leads to new multidisciplinary interactions between the propulsion system and the lifting surfaces. These aero-propulsive couplings can be leveraged to enhance the overall capacities of the aircraft. In order to do so, they must, however, be well estimated during early design phases. To address this purpose, an aerodynamic modeling is proposed and built in Python. The module makes use of a post-modified Vortex Lattice Method. For validating the proposed modeling, several flight cases are faced against a Reynolds-averaged Navier Stokes flow solver. The chosen aircraft is the NASA's experimental X-57 Maxwell. Results prove to be sufficiently good for the use during preliminary design phases. In particular, for the powered analysis, with the propellers actively modifying the wing's aerodynamics, the lift coefficient can be estimated with a precision that is kept within 7% for all the pre-stall linear region. The computation time is drastically reduced when compared with the CFD analysis, rendering the module suitable for an OAD optimization loop.**

**Keywords: DEP, X-57, electric aircraft, propeller-wing interaction**

## Nomenclature

### Symbols

| | | |
|---|---|---|
| $m$ | = | Mass of the aircraft (kg) |
| $\rho$ | = | Air density (kg.m$^{-3}$) |
| $S_w$ | = | Wing surface (m$^2$) |
| $c$ | = | Mean aerodynamic chord (m) |
| $b$ | = | Wingspan (m) |
| $V$ | = | Airspeed (m.s$^{-1}$) |
| $V_{SR}$ | = | Stall speed (m.s$^{-1}$) |
| $T$ | = | Thrust (N) |

*Ph.D., david.planas-andres@isae-supaero.fr
†Researcher engineer, eric.nguyen_van@onera.fr
‡Research engineer, carsten.doll@onera.fr
§Professor Researcher, philippe.pastor@isae.fr

DOI: 10.13009/EUCASS2023-560

| | | |
|---|---|---|
| $P$ | = | Power (W) |
| $\alpha$ | = | Angle of attack (°) |
| $\beta$ | = | Side-slip angle (°) |
| $\gamma$ | = | Flight path angle (°) |
| $\boldsymbol{\omega}$ | = | Angular velocity in body frame (rad.s$^{-1}$) |
| $\delta_a$ | = | Ailerons deflection (°) |
| $\delta_e$ | = | Elevator deflection (°) |
| $\delta_R$ | = | Rudder deflection (°) |
| $\delta_f$ | = | Flap position (°) |
| $\delta_x$ | = | Thrust setting of the HLPs (-) |
| $C_L, C_D, C_Y$ | = | Lift, drag and lateral force coefficients (-) |
| $C_l, C_m, C_n$ | = | Roll, pitch and yaw moment coefficients (-) |
| $n$ | = | Propeller angular speed (rad.s$^{-1}$) |
| $D_p$ | = | HLPs diameter (m) |
| $N_p$ | = | Number of propellers |
| $M$ | = | Number of Mach (-) |
| $Re$ | = | Number of Reynolds |

**Sub- and Superscripts**

| | | |
|---|---|---|
| $SR$ | = | Stall |
| $w$ | = | Wing |
| $p$ | = | HLP propeller |
| $T$ | = | Thrust |
| $MAX$ | = | Maximum |
| cr | = | Cruise |

**Acronyms**

| | | |
|---|---|---|
| DEP | = | Distributed Electric Propulsion |
| HLP | = | High Lift Propeller |
| HTP | = | Horizontal Tail Plane |
| MDO | = | Multidisciplinary Optimization |
| VLM | = | Vortex Lattice Method |
| RANS | = | Reynolds-Averaged Navier Stokes |

DOI: 10.13009/EUCASS2023-560

# I. Introduction

Distributed Electric Propulsion (DEP) represents a disruptive and emerging technology with promising potential to reduce energy consumption and emissions [1]. Leaving aside these ecological benefits, maybe the greatest benefit when employing this kind of concept is to exploit the novel multidisciplinary interactions that appear between the propulsion system and the lifting surfaces. Through an adequate preliminary design and analysis, these aero-propulsive synergistic effects can be exploited to increase the overall robustness, capacities, and system efficiency [2].

Perhaps, one of the most interesting ways to exploit the aero-propulsive coupling is to augment the general lift of the wing. General aviation aircraft usually have wings larger than required for cruise, as they need to meet the required stall speed fixed by regulation. When blowing onto a wing, the increased dynamic pressure in the washed zone of the wing behind the propeller increases the wing loading and therefore allows to reduce the wing surface, optimizing the wing for the cruise while still meeting the required stall speed [3]. This region behind the propeller is usually known as propeller slipstream [4]. Propellers designed with this purpose in mind are often referred to as High Lift Propellers (HLPs) and have been successfully demonstrated in aircraft concepts such as the NASA X-57 Maxwell [5] or ONERA AMPERE's concept [6]. In the case of AMPERE, this increased lift eliminated the need for flaps, eliminating an entire mechanism.

Within this context, a mid-fidelity tool able to quickly estimate the aerodynamic forces and moments while taking into account the effects of the aero-propulsive interaction would be useful for the preliminary design and analysis of this kind of aircraft. The effects of the aero-propulsive interaction cannot be properly captured by analytical or traditional empirical methods. The use of higher-fidelity methods offers good results but is dismissed at such early stages due to its large computational times. For instance, some of the CFD analyses that will be used here for comparison have computation times in the order of days, while requiring hundreds of cores. A quick estimation of these forces and moments would also open the door to an eventual multidisciplinary optimization (MDO), where computation time is even more critical. Such optimization could be aimed at improving the wing loading over the wing, reducing its size and weight, and dimensioning the size of the different involved batteries and fuel cells. Indeed, if these parameters are to be quickly mapped within the iterative design, a compromise to model the effects of the aero-propulsive couple is needed. As a result, other approaches have appeared to model the interaction between the wing and the propeller. Especially popular is the use of surrogate models extracted from wind tunnel or CFD analyses, or simple analytic methods combined with Vortex Lattice Method (VLM) tools. Among these are Jameson [7], [8], Obert et al. [9], Patterson et al. [10][11], Witkowski [12], Cho and Cho [13], Ferraro et al. [14], Veldhuis [15] or Bohari [16]. Some of these works focus on individual aspects of the interaction, or in estimating the emerged increase in performance. Generally, it is possible to evade higher fidelity methods if the drag is not involved in the optimization objective, but a minimum accuracy in its computation is needed if the aircraft is to be trimmed.

To address this purpose, an aerodynamic modeling is proposed and built in Python. The module makes use of a pre-generated aerodynamic database produced with a Vortex Lattice Method (VLM). The aerodynamic coefficients are later treated and modified through several surrogate models to account for the aero-propulsive interaction. For validating the proposed modeling, two aerodynamic analyses conducted by NASA on the X-57 experimental aircraft are chosen. The X-57 mounts twelve electric propellers in the wing's leading edge, meant to act as high lift propellers (HLP), providing propulsion and augmented lift during take-off and landing procedures. The module's results are faced against two Reynolds-averaged Navier Stokes (RANS) flow solvers, for four different flight conditions [17], [18]. The first one comprises several different flying conditions including a regular cruise case, whereas the second one tackles a given point within a landing procedure, where the deployment of a Fowler flap together with the augmented lift capacities supplied by the aero-propulsive interaction are meant to provide the required lift. Results prove to be sufficiently good for the use of this modeling for preliminary design and analysis purposes. In particular, for the powered analysis, the lift coefficient can be estimated with a precision that is kept within 7% for all the pre-stall linear region. The computation time is drastically reduced when compared with the CFD analysis, rendering the module suitable for an Overall Aircraft Design (OAD) optimization loop.

This paper is organized as follows. In section II it is explained how the general model has been built for the estimation of the aerodynamic forces and moments of a DEP aicraft with propellers mounted in front of the wing. Section III introduces the reference aircraft used within this work, presenting the modeling of the general aerodynamics of the airplane, the airfoil-related aerodynamics, and the propulsion modeling. Finally, the model is validated in section IV. Section V presents some conclusions and future guidelines of the study.

DOI: 10.13009/EUCASS2023-560

# II. General proposed modeling

The following section introduces the proposed modeling. It is explained how the model is built, which are the different software utilized, which is the logic behind the choices made, and the general advantages and drawbacks.

When building the aerodynamic database of an aircraft, different types of methods are available. The suitability of a method is usually discussed depending on its accuracy and computation time. Methods can be separated into analytical, empirical or semi-empirical, and numerical. Another important aspect is if the analyzed configuration can be considered conventional, which eases the construction of the aerodynamic database, or on the contrary, it is unconventional. Analytical and empirical or semi-empirical methods are usually developed on a database of conventional aircraft, rendering them inadequate for unconventional configurations. On the other hand, numerical methods require as input a roughly detailed geometry to build up a mesh to compute the different magnitudes. The complexity of these methods goes from a simple VLM with computation times in the order of minutes, to complex CFD-RANS analysis with considerable pre and post-processing times and computational costs.

Regarding DEP aircraft, although the majority of these concepts emerged from a baseline which is a conventional aircraft, the influence of the aero-propulsive interaction on the aerodynamics of the aircraft is sufficiently important to dismiss the conventionality. In addition, analytical or traditional empirical methods fail to capture these coupling effects. Therefore, DEP aircraft cannot just be regarded as a conventional configuration. They could be considered, however, weakly-unconventional configurations [19]. This would allow the computation of an aerodynamic database with some generic method, but a modification and post-treatment of the data are required.

A first version of a modeling was initially developed by Nguyen Van et al. This first version was used to show several DEP capabilities. In particular, it was proven the feasibility of providing lateral control through differential thrust thanks to the faster response of electrical engines [19],[20]. This allows the reduction of the vertical tail and the associated friction drag and mass. A more evolved version, including a propeller wing-interaction model, was also used for the evaluation of DEP aircraft flight envelopes [21]. The model has been extended to include some of the effects of the aero-propulsive coupling on the longitudinal dynamics of the aircraft, regarding the interaction of the HTP, and on the lateral dynamics, through the propagation of the interaction effects. Since the beginning, a requirement for the modeling was to keep a very low computation time. The modeling is meant to be used within FAST-OAD [22] (Future Aircraft Sizing Tool - Overall Aircraft Design), a package for the preliminary design, analysis, and optimization of aircraft. Therefore, the modeling has to be used within each iteration to analyze the different configurations inside an iterative design of a multidisciplinary optimization loop.

Regarding this eventual optimization, the computation of the aero-propulsive interaction within an iterative design is troublesome. The propeller slipstream interacts with a wing, that, in addition, may be flapped, and also with the horizontal tail plane (HTP), influencing considerably the trim of the aircraft. Modeling these effects is critical to correctly evaluate the aircraft performances, especially during take-off and landing approach. On one hand, enough computational speed is required to quickly re-compute the aircraft aerodynamics for any change in the geometry inside the iterative design. On the other, an adequate degree of fidelity is needed to keep the results acceptable for a preliminary phase framework. A certain degree of flexibility is also valued since this allows interfacing the modeling with other preliminary aerodynamic tools. All these reasons motivated the choice of a modified-VLM approach.

The VLM is computed with OpenVSP [23], a mid-fidelity tool for preliminary aerodynamic analysis. A pre-generated aerodynamic database, consisting of the stability derivatives, and the lift and drag distributions over the wing, is retrieved. The lift distribution is computed for two different angles of attack in order to compute the spanwise lift coefficient $C_{l_\alpha}$ and the zero-lift angle of attack $\alpha_0$. In order to consider the aero-propulsive coupling, an actuator-disk-based method proposed by Patterson et al [11], is used to modify the lift distribution extracted from the VLM. The method accounts for the increase in dynamic pressure that exists in the slipstream region and for the modification of the angle of attack seen by the wing portions behind the propeller. This augmentation of the local velocity in the slipstream leads to a lift enhancement and to a delayed stall through an increase of the local Reynolds number. Blowing into a wing usually increases the efficiency of the deflective elements behind the wing, like flaps or ailerons. To estimate this increase in performance, the method has been modified. The method, however, dismisses the swirl velocity component and its effects, since it is considered a secondary effect with respect to the increase in dynamic pressure.

DOI: 10.13009/EUCASS2023-560

A momentum theory model presented by McCormick [24], is used to estimate the speed behind the propeller, which is an input to the model. The amount of thrust depends on the modeling chosen for the propeller and will be presented later once the reference aircraft has been introduced.

In order to compute airfoil-related characteristics, XFOIL [25] and Javafoil are used. In particular, to calculate the stall characteristics and the change in the airfoil lift coefficient produced by the flap. Finally, the drag is formed by the addition of several different components. In order to compute the induced drag, the modified lift distribution is used as an input for an altered lifting line theory, see Jameson et al. [26]. Regarding the friction drag, the unblown component is computed with the VLM results, while the increase due to the augmented dynamic pressure is added later. A final component to add is the "washed" drag, which is due to the deflection of the lift caused by the slipstream, which is computed locally.

A second method, proposed by Obert et al. [9],[27] is implemented within the module, in order to evaluate the effects of the coupling on the trim of the aircraft, through estimation of the pitching moment and the performance of the HTP under the disturbed downwash. In particular, the method allows to evaluate the change in the tail-off pitching moment, with flaps retracted and deflected, the slipstream position with respect to the HTP, to measure the effects on the average dynamic pressure and the wet area, and the change in the average downwash angle due to the slipstream effect, which affects the HTP and affects the pitch moment.

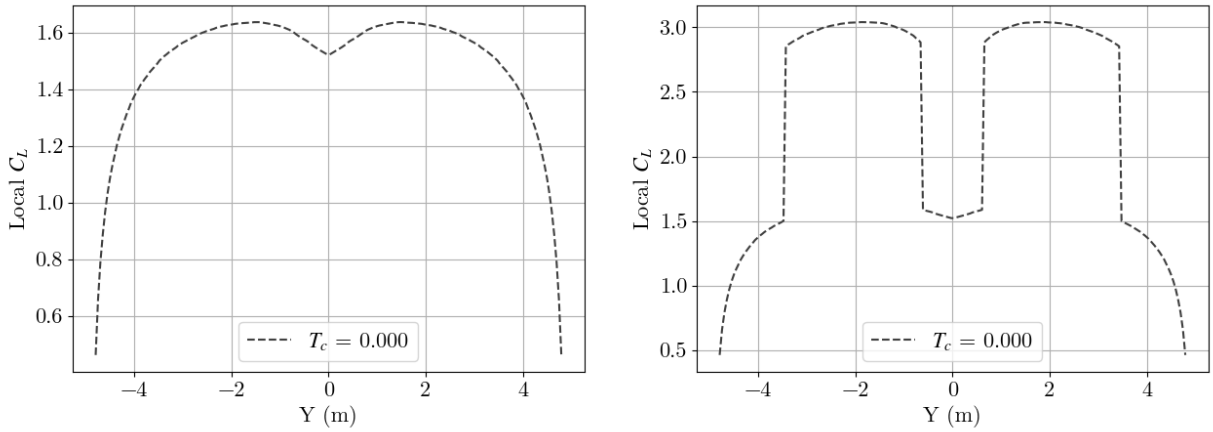


**Fig. 1 Lift distribution $C_L(y)$ for a clean configuration (left) and with the flap deployed (right), in a generic flight situation.**

The proposed modeling presents several advantages. First, the aerodynamic database generated with the VLM does not need to be recomputed as long as the wing geometry is not modified. The propeller's configuration, on the other hand, can be freely changed, whether in the number of propellers, their size, or their position in the wing, without affecting the database. If the wing is changed, the low computation time of the method does not represent a significant increase in computation when compared with the computation time of the VLM itself. The resultant model is therefore both flexible and extremely low time-consuming. The whole method is built and assembled within a module in Python.

Figure 1 shows the clean lift distribution and the resultant lift distribution when deploying the flap to 30 °, respectively. Note that both the augmentation of lift due to the flap and the aero-propulsive interaction are done locally, over the affected span stations, influencing the results. For further information about the proposed modeling, the reader is referred to [21], [19], and [28].

DOI: 10.13009/EUCASS2023-560

## III. Modeling of the chosen referenced aircraft

So far, the presented model is valid for any weakly unconventional configuration with propellers mounted in front of the wing. This section particularizes the model for a chosen reference aircraft regarding the airfoil and general aircraft aerodynamics, and the propulsion modeling. The X-57 Maxwell from NASA is the aircraft chosen for the validation of the model. NASA's X-57 is an all-electric experimental aircraft designed to demonstrate multiple leading-edge technologies, in particular, that an all-electric airplane can be more efficient, quieter, and more environmentally friendly than airplanes powered by traditional gas-powered piston engines [29].

The X-57 results from an extensive modification of a gas-powered Tecnam P2006T General aviation aircraft and has passed through four modification phases until the current version (Mod IV), see figure 2. The original propellers, next to the fuselage at the beginning, have been moved to the wing tip, and a total of twelve small electric motors have been installed in front of the wing's leading edge, in pods placed under the wing. These small electric engines are meant to be used as high-lift propellers, providing propulsion and augmented lift during the take-off and landing procedures. The required design stall speed $V_{SR}$ is 58 knots (29.84 m/s). Being the gross weight of 3000 lb (1360 kg), this means that the maximum lift coefficient $C_{L_{MAX}}$ should be 3.95. The X-57 has been designed to achieve this $C_{L_{MAX}}$ with the combination of a high-lift airfoil, a flap Fowler extendable until 30°, and the lift augmentation provided by the 12 HLPs. The unblown maximum lift coefficient of the high-lift wing with the 30° flap setting is 2.439, so the HLPs should be able to give the remaining 1.5. The augmented lift has hence allowed reducing the size of the wing to 42% of the original size, which results in a larger wing loading, $W/S_W$.

Whereas the two bigger, outer propellers serve as propulsors during the cruise stage, the twelve small HLPs are meant to be operative just during the high lift-required stages, around take-off and landing, and after that, they can be turned off and folded back to reduce their associated drag. This aircraft has been chosen due to several reasons:

- The model implemented relies for certain calculations on a surrogate model presented by Patterson [11], which was originally proposed for a quickly-estimation of DEP augmented lift capacities during the design of the X-57.
- NASA's X-57 is a DEP demonstrator with several inner propellers specifically designed and meant to act as HLPs. They are placed in front of the wing and interact, therefore, with the wing system through the main mechanism of the Propeller-Wing interaction, the slipstream effect.
- There is a large amount of published and publicly available documentation, and the interest of the project has always been to share knowledge in order to be helpful for future engineers interested in designing all-electric air vehicles [29].

Regarding the last bullet point, this paper particularly relies on two published analyses for validating the proposed modeling, where RANS methods are utilized to compute the results. The general characteristics of the X-57 are shown in table 1. All the related published NASA documents referenced in this document can be found in the NASA repository for X-57 publications [30].

**Fig. 2 NASA's X-57 Mod IV**

DOI: 10.13009/EUCASS2023-560

**Table 1 X-57 general characteristics**

| Parameter | Value |
|---|---|
| Wingspan: $b$ (m) | 9.642 |
| Wing surface: $S_w$ ($m^2$) | 6.196 |
| Overall Length (m) | 8.75 |
| Mass: $m$ (Kg) | 1360 |
| Mean aerodynamic chord: $c$ (m) | 0.649 |
| Ref. cruise speed (m/s) | 77 |
| HLPs power (kW) | 10.5 |
| Cruise Propeller power (kW) | 60.08 |
| Horizontal Tailplane area ($m^2$) | 2.452 |
| Vertical Tailplane area ($m^2$) | 3.902 |
| Number of HLPs: $N_p$ | 12 |
| HLPs Diameter: $D_p$ (m) | 0.5758 |

### A. General aircraft aerodynamics

For the general aerodynamics, as explained, a pre-generated aerodynamic database is produced with the solver OpenVSP [23]. The geometry used is available at the OpenVSP Hangar [31]. The geometry corresponds to the X-57 Maxwell MOD IV, but here it has been simplified by removing all the engine's (HLPs and cruise) propellers, spinners, nacelles, pylons, and the landing gear pod. The geometry used is shown in figure 3. Regarding the aerodynamic database generated, OpenVSP is capable of computing the following stability derivatives for a given flight condition:

$$C_L, C_D, C_Y, C_l, C_m, C_n = f(V, \alpha, \beta, p, q, r, \delta_a, \delta_e, \delta_r) \tag{1}$$

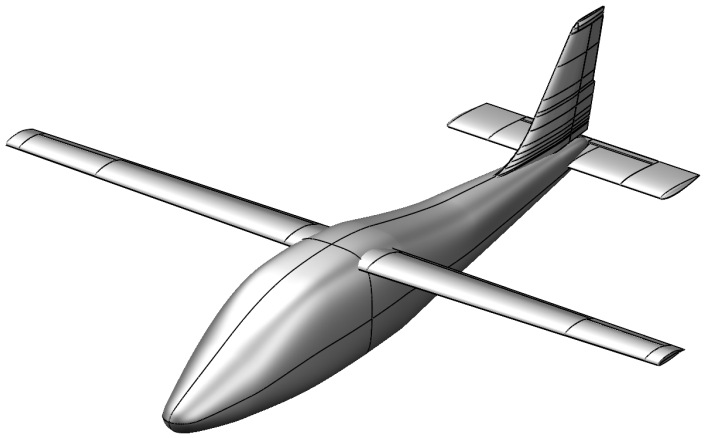

**Fig. 3 X-57 simplified geometry model used in OpenVSP**

As previously explained, the lift distribution, $C_L(y)$, is also derived from the VLM. The lift distribution is computed for two different angles of attack and is used as an input for the actuator disk-based method that computes the augmented lift that results from the interaction. This lift distribution is also used for the calculus of all the induced drag, the augmented friction drag, and the washed drag.

DOI: 10.13009/EUCASS2023-560

### B. Airfoil and Flapped airfoil modeling

The model relies on airfoil preliminary analysis to compute some of the aerodynamic characteristics and bounds. In particular, the stall angle of attack $\alpha_{SR}$, the post-stall drag, and the airfoil augmented lift coefficient when deploying the flap $\Delta C_{l,\ fl}$, are computed with airfoil analysis. The airfoil used in the X-57 has been named "GNEW5BP93B". It is a high-lift cruise airfoil and has been specifically designed for the demonstrator. The information regarding its design and analysis is available in [32]. The explicit grid coordinates of the airfoil have not been, however, published. In order to obtain the airfoil geometry to work with, the airfoil has been digitized and approximated coordinates have been computed. The resultant airfoil's profile can be seen in figure 4, with the flap Fowler retracted and deployed to 30 °.

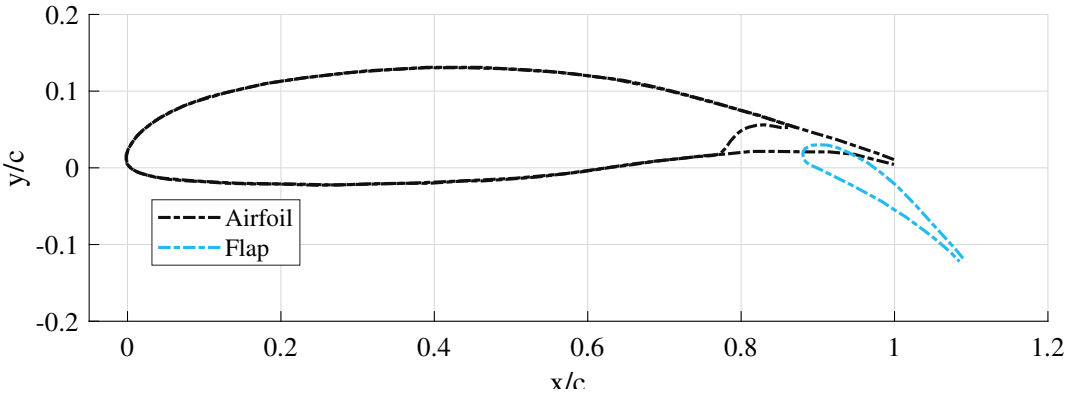


**Fig. 4 GNEW5BP93B Airfoil digitized profile**

The airfoil has been consequently analyzed with XFOIL [25], or with Javafoil [33] for the deployed-flap configuration, since XFOIL can not handle multi-elements. Results are confronted with the ones published in [32], computed with MSES, a coupled viscous/inviscid Euler method for 2-D analysis. For the flap's retracted cases, analyses are computed at cruise condition ($M = 0.233, Re = 2.35e+06, N_{crit} = 9$), whereas, for the cases with the flap Fowler deployed to 30 degrees, the condition computed is close to a landing or climbing procedure ($M = 0.096, Re = 1e+06, N_{crit} = 9$). The boundary layer laminar-turbulent transition, which has been observed in [32] to occur at the 69% of the chord in the upper surface and at the 62% in the lower surface, has not been forced in the XFOIL analysis shown below. For the model, in order to maintain coherence, it is, however, forced at 10% of the chord to account for the injection of kinetic energy passed to the flow from the slipstream of the propeller.

Results for the airfoil lift, drag, and pitch moment coefficients are shown in figures 5, 6, and 7. For the XFOIL analysis with flaps retracted, results match certainly well with [32], and there are just slight differences in the case of $C_L$ and $C_D$ for high angles of attack, outside the linear region, which is of no interest. For the Fowler flap analyzed with Javafoil, results differ vaguely more, but tendencies are reasonably well captured.

DOI: 10.13009/EUCASS2023-560

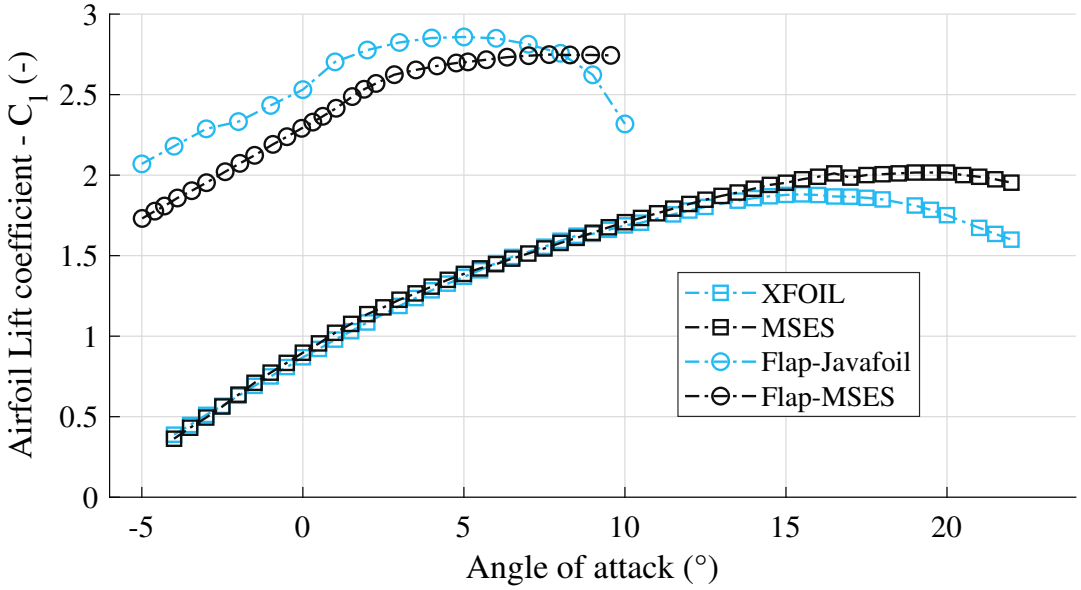


**Fig. 5 Comparison of GNEW5BP93B lift coefficient $C_L$**

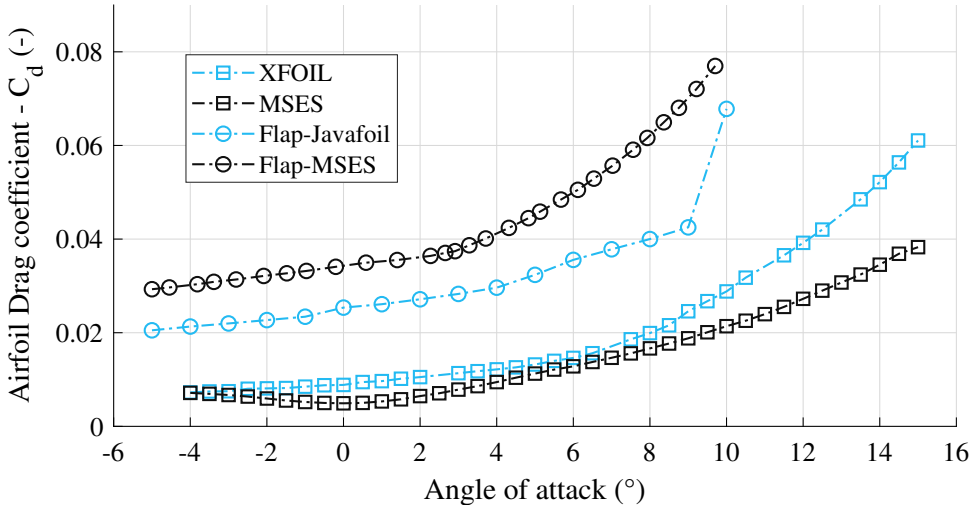


**Fig. 6 Comparison of GNEW5BP93B drag coefficient $C_D$**

DOI: 10.13009/EUCASS2023-560

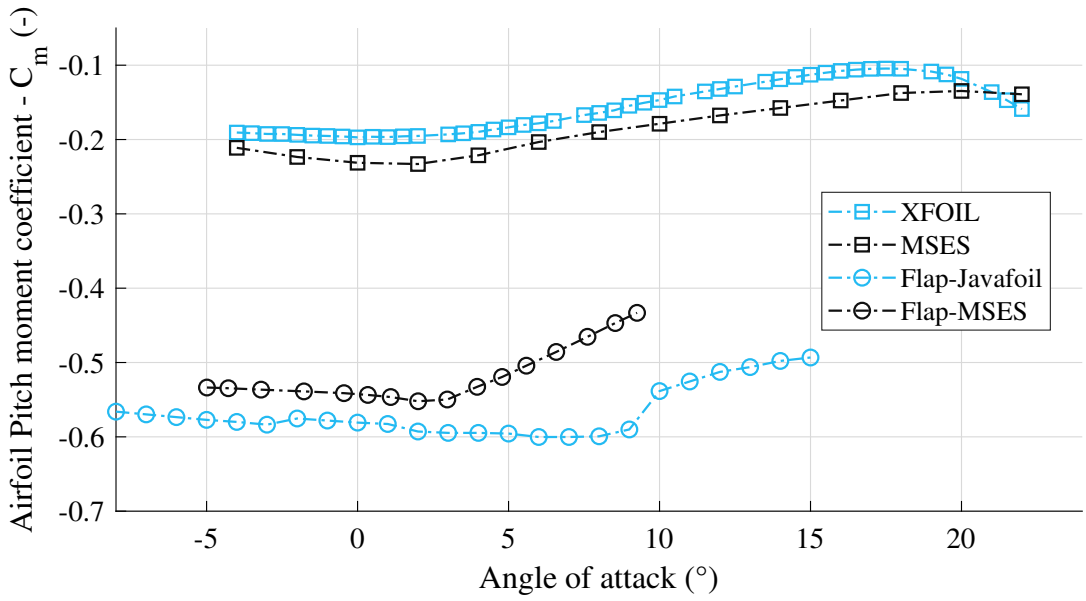


**Fig. 7 Comparison of GNEW5BP93B moment coefficient $C_M$**

### C. Thrust modeling

The general idea of this study is not to validate a thrust model, but an aerodynamic one. Thrust is, however, an input to the aerodynamic model, as it is responsible for generating the slipstream. The mechanism of connection between the thrust and the aero-propulsive interaction is the speed produced past the propeller, $V_P$. This speed is very simply calculated through the momentum theory derived by McCormick [24].

$$T = 2\rho S_p V_{ep} V_p \tag{2}$$

Where $V_{ep}$ is the resultant speed from summing the freestream speed and the speed past the propeller:

$$\boldsymbol{V_{ep}} = \boldsymbol{V_\infty} + \boldsymbol{V_p} \tag{3}$$

Therefore, and since the model is meant to be validated in specific flight points, the modeling is entirely based on the data available. For the HLP, these are the $C_T - J$ curve, provided in [34] and plotted in figure 8. The original HLPs in the X-57 are designed to achieve a specific and uniform through-the-blade induced axial speed at the desired stall speed condition, at 58 knots. For computing the thrust of each propeller in different flight conditions, the data presented in [34] are used for building the propellers thrust and power coefficients versus the advance ratio charts: $C_T = C_T(J)$ and $C_P = C_P(J)$. The total maximum power of the set of HLPs is ($P = 12 \times 10.5\,kW = 126\,kW$, see table 1). For a given airspeed $V$ and a propeller thrust setting $\delta_{x,i}$, the propeller angular speed $n$ is computed through iteration between the amount of available power and the propeller power coefficient chart :

$$P_i = \frac{P}{N_p}\,\delta_{x,i} = \rho\, n^3\, D_p^5\, C_P\,(J) \tag{4}$$

Once $n$ has been found, the thrust can be computed with $C_T\,(J)$.

DOI: 10.13009/EUCASS2023-560

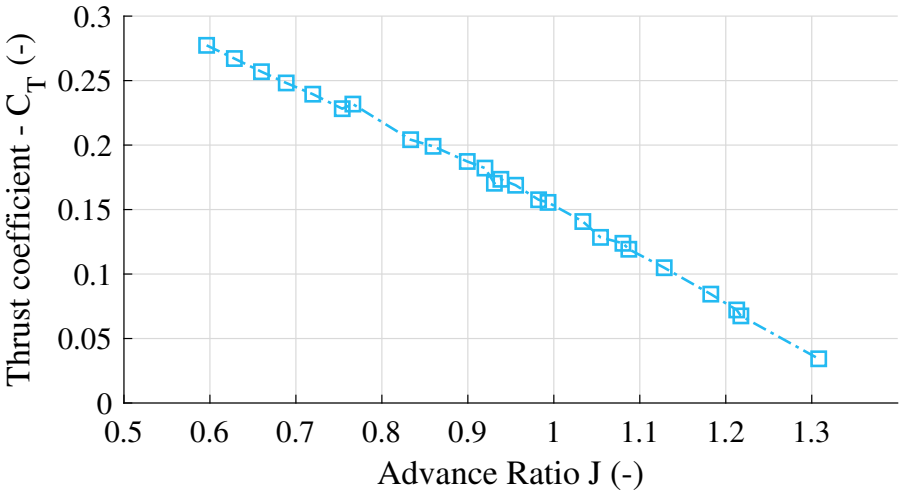


**Fig. 8 Thrust coefficient $C_T$ versus advance ratio $J$ for the X-57 high lift propellers**

For the cruise propellers, thrust is computed with a common thrust model proposed by Sachs, 2012 [35]. The thrust of one propeller is:

$$T = \frac{P_{E_{MAX}}}{N_m} V^{-1} \eta_{tot} \delta_x = M_{t_{MAX}}\ n\ V^{-1} \eta_{tot} \delta_x \tag{5}$$

Where $P_{E_{MAX}}$ is the total electric power available from the line, $N_m = 2$ is the number of engines, $\eta_{tot}$ is the total efficiency of the propellers plus the engines, $M_{t_{MAX}}$ is the cruise propeller maximum continuous torque, $n$ is the angular speed, and $\delta_x$ is the thrust setting. By knowing the cruise drag coefficient [36], $C_{D,cr} = 0.05423$, drag and thrust (which are equal due to the zero propeller's installation angle and wing tilt) can be solved:

$$T_{cr} = D_{cr} = \frac{1}{2} \rho V_{cr}^2 S\ C_{D,cr} \tag{6}$$

Finally, by knowing the maximum torque $M_{t_{MAX}} = 255\ Nm$, and the cruise propeller torque at cruise $M_{t,cr} = 177\ Nm$, and taking into account that the propeller angular speed is the same in the two cases (n = 2250 = 235.62 rad/s) [37], the cruise thrust setting can be solved $\delta_{x,cr} = 69.4\%$. For the cruise, this yields a total engine and propeller efficiency $\eta_{tot,cr} = 0.8826$. Although this value is considered constant, and therefore $\eta_{tot} = \eta_{tot,cr}$, the propeller efficiency does depend on the advance ratio $J$, and therefore this approach will be accurate just around the cruise point. The maximum continuous power required by the propeller is easily computed as the product of the maximum continuous torque and the propeller angular speed at that condition $P_{p_{MAX}} = M_{t_{MAX}} * n = 60.082\ KW$, therefore the total electric power available must be $P_{E_{MAX}} \geq N_m\ P_{p_{MAX}}$.

DOI: 10.13009/EUCASS2023-560

# IV. Validation of the proposed modeling: Results

The following section addresses the validation of the built numerical model. This work relies on two published works for the validation of the presented modeling. The first one is a computational analysis of the aerodynamics of the unpowered X-57 Mod-III [17], meaning that high lift (and also cruise) propulsors are inoperative during the analysis. The second one is a computational analysis of the aerodynamics of the Mod-IV including the HLP propulsors and, therefore, the aero-propulsive interaction, together with flap deflection [18]. The differences between the Mod III and IV are minimum and they are just limited to the addition of the HLP propellers to the already-existing nacelles in the Mod III version. The Mod IV is shown in figure 2. A RANS flow solver, called Launch Ascent Vehicle Aerodynamics (LAVA), is used in these analyses to compute the longitudinal forces and moment coefficients for a wide range of angles of attack.

Due to the nature of the X-57, its operation, and the available results, four flight points are analyzed and explored within this validation. The first three cases consist of unpowered conditions at both the cruise point and low-altitude and low-speed points, with all the engines shut down. The last case consists of a low-speed high-lift condition immediately after take-off with the HLPs operating. Although the aero-propulsive interaction is just taking place at the last one of these flight conditions, analyzing and comparing results for the conditions without interaction is also interesting since the numerical tool built for modeling the interaction uses the unpowered aerodynamics as a starting point and modifies the unpowered lift and drag coefficients of the lifting surfaces. To mention that the results include as well the post-stall region estimation, in the case of the lift and pitch moment coefficient. Regarding the drag coefficient, results after stall quickly diverge from the model, and are not shown. Generally, the post-stall is a region of no interest and the estimation of the forces in this region was never the aim of the modeling, since it is intended to trim the aircraft or to analyze the performance for regular flight conditions. The stall progress and limit are however of interest in order to know the operational limits of the aircraft. A general summary of the conditions of the four compared cases is shown in table 2.

**Table 2 Flight cases validated**

| **Unpowered conditions** | | | | |
|---|---|---|---|---|
| **Numbering** | **Altitude (m)** | **Mach** | **HLPs Thrust setting** (%) | **Flap Deflection** (°) |
| 1 | ≃ 2500 | 0.233 | 0 | 0 |
| 2 | ≃ 750 | 0.149 | 0 | 10 |
| 3 | ≃ 750 | 0.119 | 0 | 30 |
| **High-lift Powered condition** | | | | |
| 4 | ≃ 750 | 0.119 | 39 | 30 |

### A. Cases 1-3: Unpowered conditions

The first case explored is an unpowered flight condition on a regular cruise. The design cruise condition is 150 KTAS (77.17 m/s) at 8000 ft (≈ 2440 m). This yields a cruise lift coefficient $C_{L_{cr}}$ of 0.75 for an angle of attack $\alpha$ of 0 degrees. During the cruise, the HLPs are turned off and their blades are folded back, being operative just the two outer cruise propellers. These propellers can, therefore, provide a reduction of the induced drag $C_{D,i}$ by reducing the vortex tip of the wing when counter-rotating to it, but their effect in the wing's lift can be neglected due to the natural elliptical lift distribution where no lift is produced on the tips. This reduction of the induced drag is not computed in the model developed, as it is derived from the swirl interaction, but the results used for comparison are in any case for an unpowered situation with all engines shut down, so this reduction of the induced drag by counter-rotation to the vortex tip is not taking place.

The results computed are the longitudinal forces and moments coefficients: $C_L, C_D, C_m$. The lift, drag, and pitch moment coefficients are computed in the airspeed frame and faced against the angle of attack. These results are compared with the ones presented in [17], a computational analysis of the aerodynamics of the unpowered X-57 Mod-III. Results are presented in figure 9.

DOI: 10.13009/EUCASS2023-560

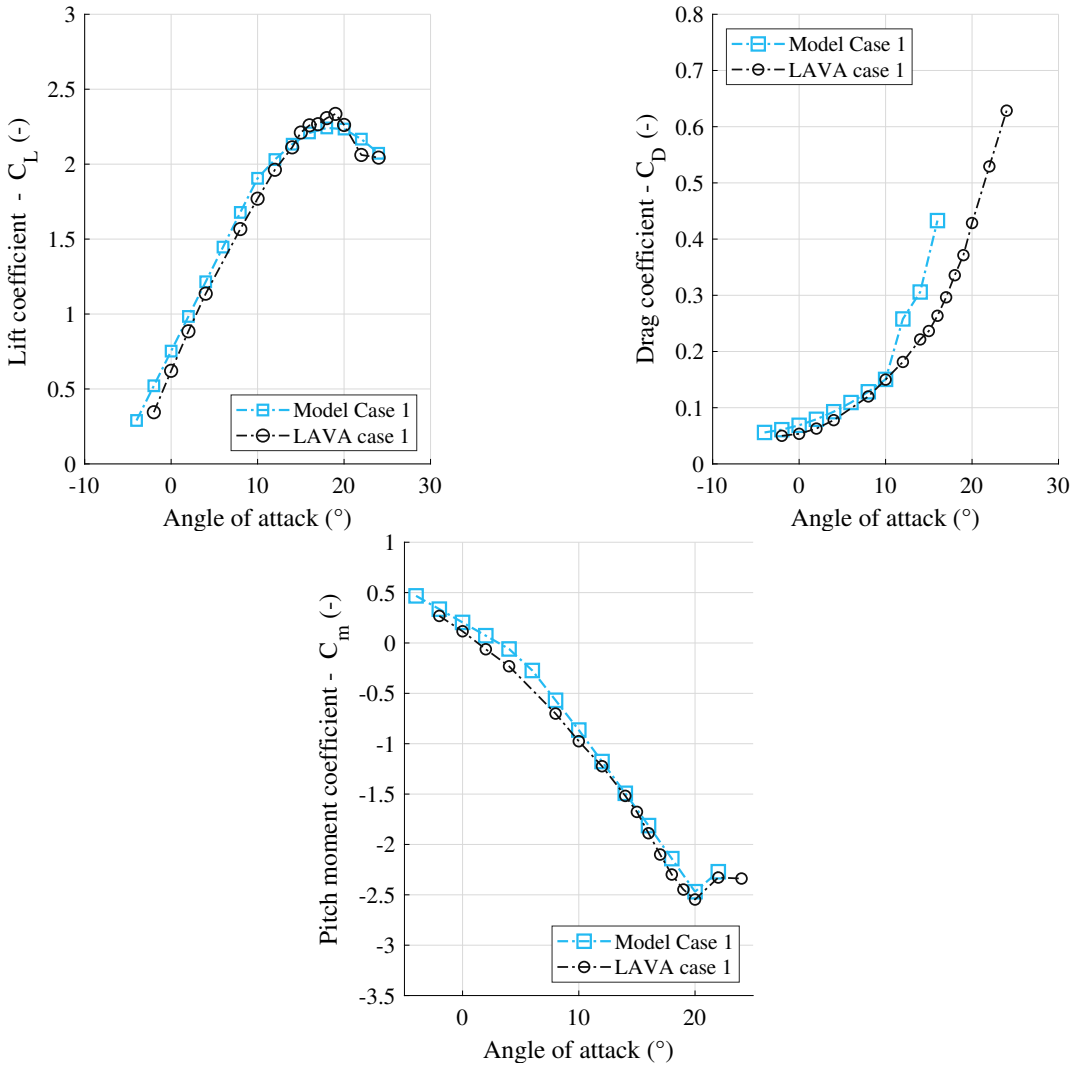


**Fig. 9 Comparison of results between [17] and the proposed modeling, for case 1, for the lift $C_L$, drag $C_D$, and pitch moment $C_m$ coefficients**

For this first unblown case, results can be considered as satisfactory. For the lift coefficient, $C_L$, all the zero-angle of attack lift, $C_{L_0}$, the lift slope, $C_{L\alpha}$, and the stall progress and detachment point are fairly well estimated, with the maximum error kept under the 7 %. Regarding the drag coefficient $C_D$, results are not as good, with this coefficient well captured until $\alpha \simeq 10$ °, when the results start to diverge due to the progressive stall that starts at that point. This can be seen in the lift coefficient, where the slope begins to drop very slightly starting from that point. Finally, the pitch moment coefficient is satisfactorily well estimated when regarding all the zero-angle of attack pitch moment $C_{m0}$, the slope, and the detachment of the flow on the HTP.

The second case explored and compared is a low-altitude and low-speed condition. The Fowler flap is not fully deployed for this case, but extended to a third of its maximum deflection, 10°. On the other hand, the analysis is once again unpowered, meaning that both the HLPs and the cruise propellers are shut down and do not interfere with the aerodynamics of the aircraft through any propulsion mechanism. The condition can be seen as an intermediate point at the descent where the cruise propellers have already been turned off in order to reduce the speed and the Fowler flap is being deployed, but the HLPs have not been turned on yet. Results can be seen in figure 10.

DOI: 10.13009/EUCASS2023-560

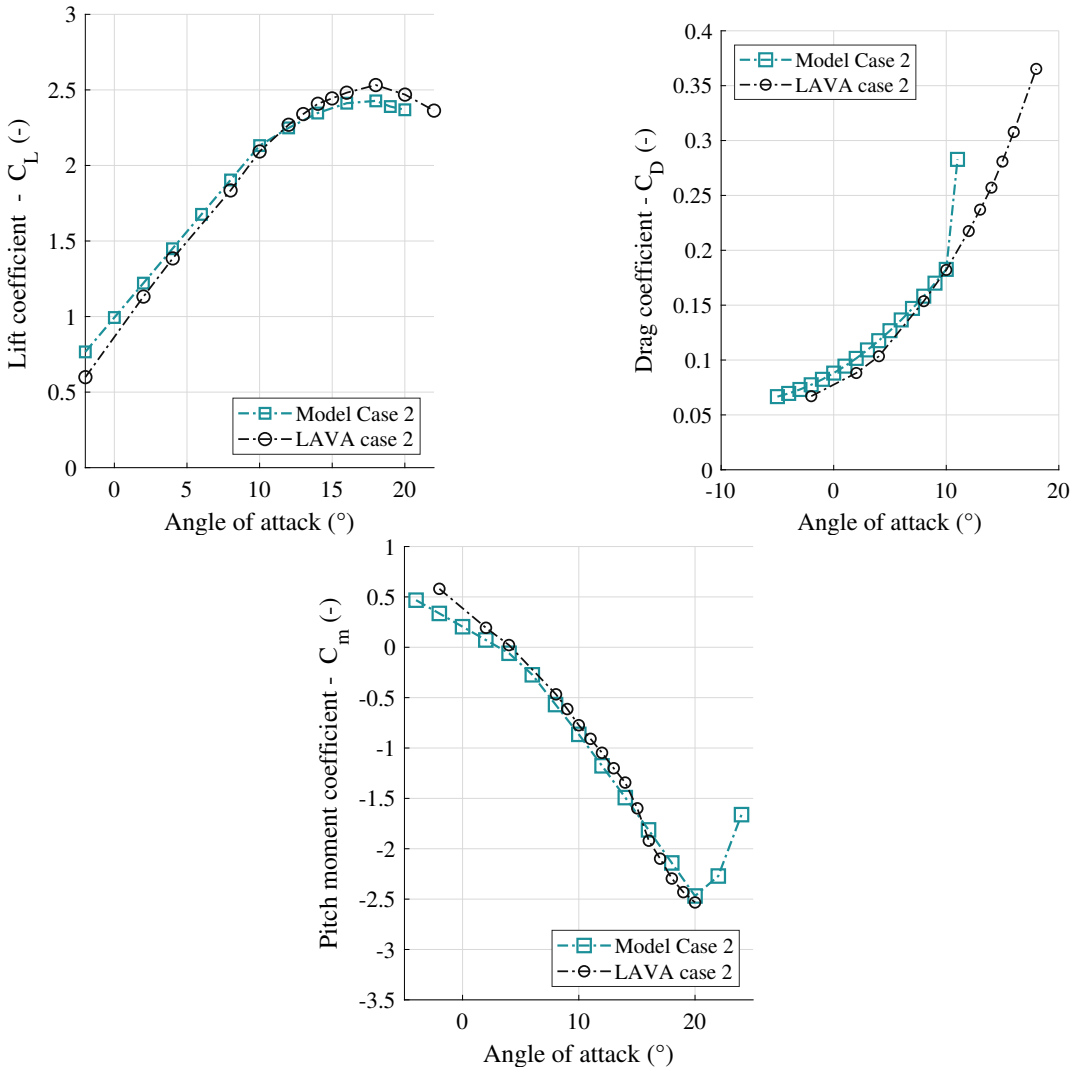


**Fig. 10 Comparison of results between [17] and the proposed modeling, for case 2, for the lift $C_L$, drag $C_D$, and pitch moment $C_m$ coefficients**

For this second unblown case, the lift coefficient, $C_L$, is in general, well estimated. The zero-angle of attack lift, $C_{L_0}$ presents some discrepancy, but the general slope of the curve is well captured. The progressive stall, which is much more smooth in this case than in the previous one, is also well estimated. To notice the change in the zero lift coefficient, $C_{L_0}$, when compared with the first case, brought up by the slight deflection of the flap, up to a third of its maximum range of deployment. Once again, due to the progressive stall that starts around $\alpha \simeq 10$ °, the drag is well captured until this point, quickly diverging once passed that limit. Lastly, the pitch moment coefficient, $C_m$, is, overall, well estimated and the curve tendency is well captured.

The third compared case represents a step further with respect to the previous one. It is, newly, a low-altitude and low-speed condition, but the Fowler flap is now deployed to its maximum deflection, until 30°. All the engines are again shut down, being the analysis still unpowered. The comparison of results for this last unpowered case is shown below, in figure 11.

DOI: 10.13009/EUCASS2023-560

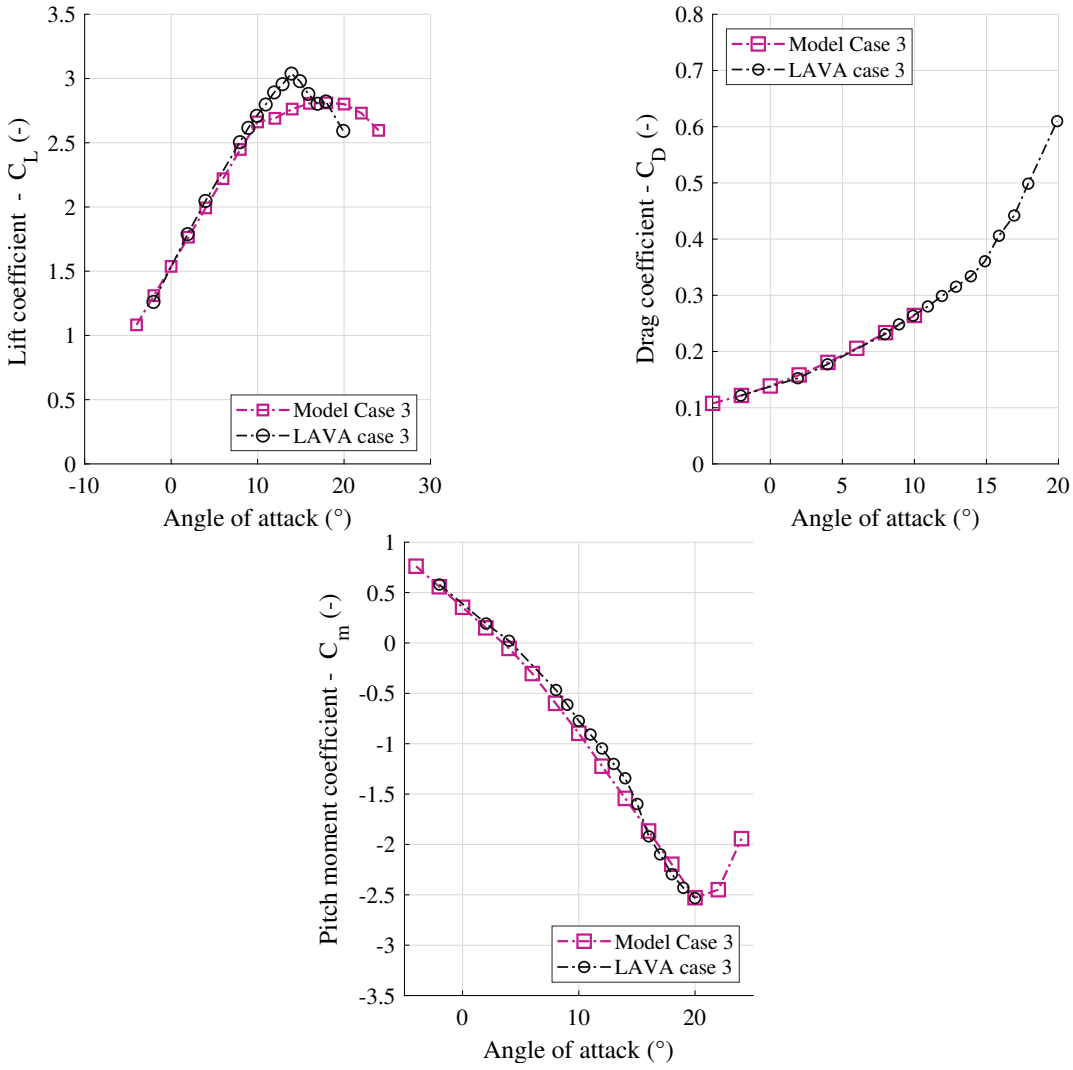


**Fig. 11 Comparison of results between [17] and the proposed modeling, for case 3, for the lift $C_L$, drag $C_D$, and pitch moment $C_m$ coefficients**

For this last case, without blowing onto the wing, results are considered, overall, good. Both the zero-angle of attack lift, $C_{L_0}$, and the lift slope, $C_{L\alpha}$, are well estimated. For this case, the stall is, however, not well captured, with the model predicting an earlier stall, and therefore starting the drop in the lift earlier. The great increase in the zero-angle of attack lift, $C_{L_0}$, caused by the full deployment of the Fowler flap is worthy of attention. The full deflection of the Fowler flap causes in this case a The drag coefficient, $C_D$, is very well estimated, with an error inferior to the 5 %, until the aforementioned estimated point of stall. The pitch moment coefficient, $C_m$, is well estimated for all the angles of attack in the wide range $-4\,^\circ < \alpha < 20\,^\circ$.

### B. High Lift condition

The last condition explored corresponds to the powered analysis of the HLPs. The HLPs must be operative in order to create the aero-propulsive interaction that allows for lift enhancement. The airspeed can not be very high, since this will reduce the ratio between the speed past the propeller and the free airspeed, and will drop the importance of the interaction and the lift augmentation. The computation analysis performed in [18] is done at 2500 ft (760 m) and 40.145 m/s, which corresponds to $M = 0.119$. For this case, the HLPs are not at their maximum setting, but operating at a 39% of their capacity. The importance of the aero-propulsive interaction is, however, remarkable, and can be seen in the lift augmentation. Results are shown in figure 12.

DOI: 10.13009/EUCASS2023-560

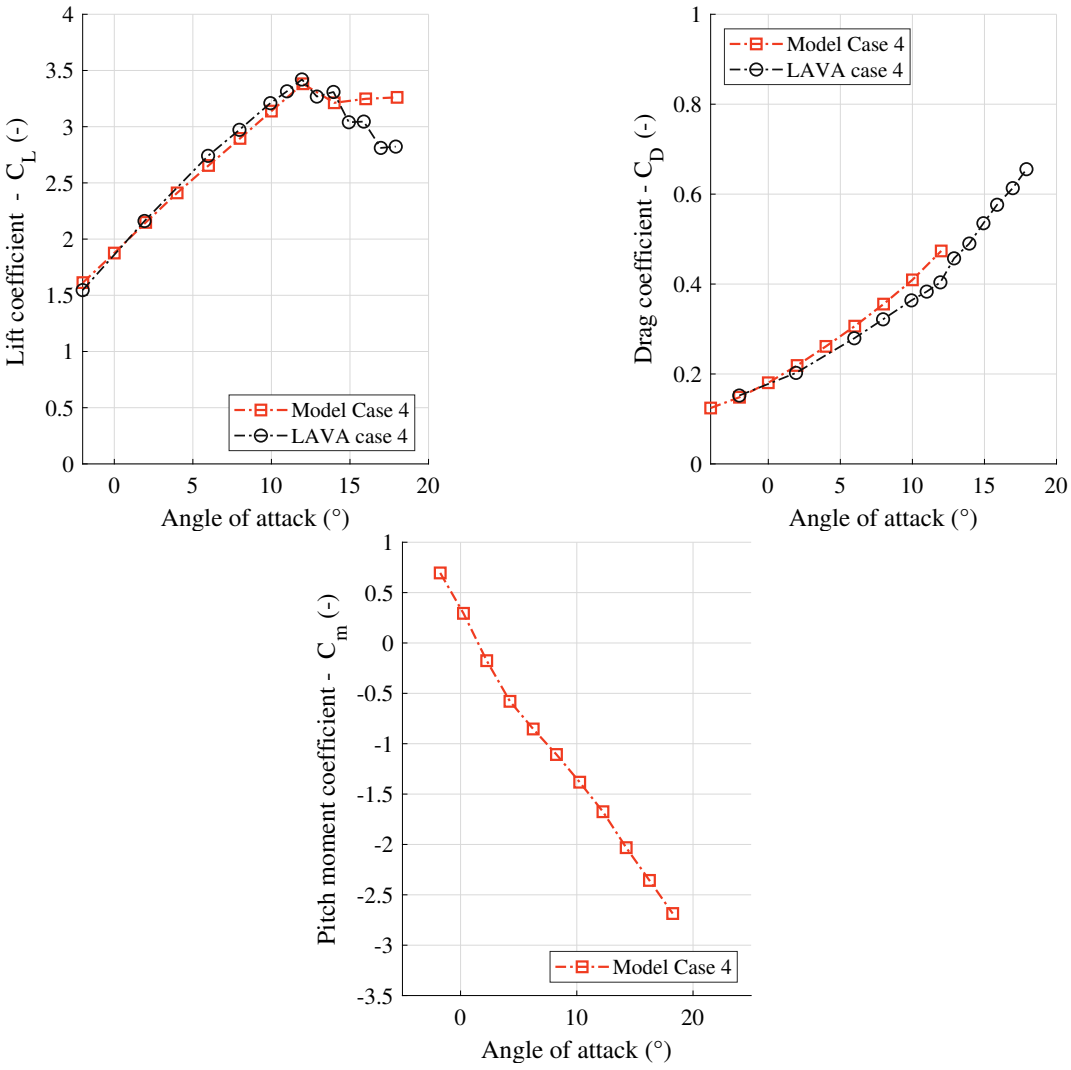


**Fig. 12 Comparison of results between [18] and the proposed modeling, for case 4, for the lift $C_L$, drag $C_D$, and pitch moment $C_m$ coefficients.**

The results from the model are positive for all the pre-stall region. Both the zero-angle of attack lift, $C_{L_0}$, and the lift slope, $C_{L\alpha}$, are well estimated for a complex case where there is blowing onto a flapped wing. The pre-stall drag is, once again, well captured, until the stall, with a maximum error of 10 % at this point. The stall point is also well estimated. Once again, the post-stall region, particularly for post-stall drag, is not well captured, but it is, as mentioned above, a region of no interest. There are no data from the RANS solver regarding the pitch moment coefficient $C_m$ for this blown case. The results from the model are, however, shown. These results are of interest due to the existing interaction of the slipstream and the HTP, which modifies the downwash over this element. This modification depends on the size of the contracted slipstream and on the relative position between the two elements, causing several changes in the slope of the pitch moment coefficient. To notice once again the increase in the lift coefficient, $C_L$ with respect to the precedent cases. The maximum lift coefficient achieved now is almost 3.5, almost 1.1 over the first case (with no flap and no blowing), and 0.5 over the third case (with the flap fully deployed). This increase is caused due to the full deflection of the Fowler flap and the blowing onto the wing. The first modifies the zero-angle of attack lift, $C_{L_0}$, and the second increases the lift slope, $C_{L\alpha}$. By blowing onto a flap its efficiency is as well increased, so the modification of $C_{L_0}$ is expected to be larger than just the pure one due to the flap deflection. As a reminder, the thrust setting of the HLPs for this case is just at 39 % of its maximum capacity, see table 2. meaning that there is still a lot of credit to be obtained from distributed propulsion and the aero-propulsive coupling in terms of lift enhancement.

DOI: 10.13009/EUCASS2023-560

## V. Conclusions

The objective of this paper was to present and validate a modeling for the quick estimation of the aerodynamic forces and moments in the presence of aero-propulsive interactions which typically take place in DEP aircraft.

The accurate estimation of these forces and moments is computationally expensive and requires large pre and post-processing times. For instance, the aerodynamic analyses conducted by NASA that were used in this paper to validate the model required around 1200 cores in order to achieve computation times of around 16 hours.

A model has been developed to address this purpose. The model has proven to be both quick and flexible, with computation times that remain in the order of seconds, thanks to the pre-generation of the VLM aerodynamic database and the implementation within Python of two surrogate methods for the estimation of the coupling effects. At the same time, the modeling has demonstrated its capacity to accurately estimate the aerodynamic forces and moments, both with and without HLPs operating, and therefore with the aero-propulsive coupling ongoing. A total of four cases have been analyzed and compared. Overall, the results can be considered as satisfactory. In the majority of cases all the lift, drag, and pitch moment coefficients are estimated with errors that are kept below 10 % with respect to the RANS methods. In particular, for the powered analysis, with the propellers actively modifying the wing's aerodynamics, the lift coefficient can be estimated with a precision that is kept within 7% for all the pre-stall linear region. For this case, the stall point is also well estimated. The post-stall estimation is an arduous task, however, and since in all cases the aircraft is to be trimmed outside of this region, this has never been one of the goals of the study.

The presented modeling is therefore suitable to be implemented within an optimization loop. With an optimum propeller geometry, installation characteristics, and distribution of power, the wing load can be increased, and the stall speed can be reduced while maintaining the same amount of power utilized, or the required stall speed can still be met while reducing the power. A study in this sense has already been done by using the presented model. The logical course of action is to consider the wing's aerodynamics in the optimization loop. By reducing the size of the wing and the installed power of the HLP's, the general weight of the aircraft can be reduced, which can be exploited for yielding a payload increase, a batteries enlargement, and an augmented range. This future step will be realized through the implementation of the developed model in an Overall Aircraft Design tool: FAST-OAD.

## VI. Acknowledgments

The author would like to thank ISAE-Supaero, Airbus in the frame of the Chair CEDAR, and the FONISEN Federation for their investment and funding in this project.

# References


[1] Hermetz, J., Ridel, M., and Doll, C., "Distributed electric propulsion for small business aircraft a concept-plane for key-technologies investigations." *ICAS 2016*, DAEJEON, South Korea, 2016. URL https://hal.science/hal-01408988.

[2] Kim, H. D., Perry, A. T., and Ansell, P. J., "A Review of Distributed Electric Propulsion Concepts for Air Vehicle Technology," *2018 AIAA/IEEE Electric Aircraft Technologies Symposium*, 2018. https://doi.org/10.2514/6.2018-4998, URL https://arc.aiaa.org/doi/abs/10.2514/6.2018-4998.

[3] Patterson, M. D., and Borer, N. K., "Approach Considerations in Aircraft with High-Lift Propeller Systems," *17th AIAA Aviation Technology, Integration, and Operations Conference*, 2017. https://doi.org/10.2514/6.2017-3782, URL https://arc.aiaa.org/doi/abs/10.2514/6.2017-3782.

[4] Obert, E., *Aerodynamic design of transport aircraft.*, IOS Press, 2009.

[5] Borer, N. K., Patterson, M. D., Viken, J. K., Moore, M. D., Bevirt, J., Stoll, A. M., and Gibson, A. R., "Design and Performance of the NASA SCEPTOR Distributed Electric Propulsion Flight Demonstrator," *16th AIAA Aviation Technology, Integration, and Operations Conference*, 2016. https://doi.org/10.2514/6.2016-3920, URL https://arc.aiaa.org/doi/abs/10.2514/6.2016-3920.

[6] Dillinger, E., Döll, C., Liaboeuf, R., Toussaint, C., Hermetz, J., Verbeke, C., and Ridel, M., "Handling qualities of ONERA's small business concept plane with Distributed Electric Propulsion," *In 31st ICAS Conference*, Belo Horizonte, Minas Gerais, Brazil, 2018.

[7] Jameson, A., "Preliminary Investigation of the Lift of a Wing in an Elliptic Slipstream." *Aerodynamics Report 393-68-6, Grumman*, 1968. https://doi.org/10.2514/6.2022-0004.

[8] Jameson, A., *Analysis of Wing Slipstream Flow Interaction.*, no. NASA CR-1632, 1970.

[9] Obert., E., "The effect of propeller slipstream on the static longitudinal stability and control of multi-engined propeller aircraft." *Delf University of Technology*, 1994.

[10] Patterson, M. D., "Conceptual Design of High-Lift Propeller Systems for Small Electric Aircraft," Ph.D. thesis, Georgia Institute of Technology, Georgia, USA, aug. 2016.

[11] Patterson, M. D., Derlaga, J. M., and Borer, N. K., "High-Lift Propeller System Configuration Selection for NASA's SCEPTOR Distributed Electric Propulsion Flight Demonstrator," *16th AIAA Aviation Technology, Integration, and Operations Conference*, 2016. https://doi.org/10.2514/6.2016-3922, URL https://arc.aiaa.org/doi/abs/10.2514/6.2016-3922.

[12] Witkowski, D. P., Lee, A. K. H., and Sullivan, J. P., "Aerodynamic interaction between propellers and wings," *Journal of Aircraft*, Vol. 26, No. 9, 1989, pp. 829–836. https://doi.org/10.2514/3.45848, URL https://doi.org/10.2514/3.45848.

[13] Cho, J., and Cho, J., "Quasi-steady aerodynamic analysis of propeller–wing interaction," *International Journal for Numerical Methods in Fluids*, Vol. 30, No. 8, 1999, pp. 1027–1042. https://doi.org/https://doi.org/10.1002/(SICI)1097-0363(19990830)30:8<1027::AID-FLD878>3.0.CO;2-R, URL https://onlinelibrary.wiley.com/doi/abs/10.1002/%28SICI%291097-0363%2819990830%2930%3A8%3C1027%3A%3AAID-FLD878%3E3.0.CO%3B2-R.

[14] Ferraro, G., Kipouros, T., Savill, M., Rampurawala, A., and Agostinelli, C., "Propeller-Wing Interaction Prediction for Early Design," *AIAA SciTech 2014 Forum*, 2014. https://doi.org/10.2514/6.2014-0564.

[15] Veldhuis., L., "Propeller Wing Aerodynamic Interference." Ph.D. thesis, Delft University of Technology, The Netherlands, 2005.

[16] Bohari, B., Bronz, M., Bernard, E., and Borlon, Q., "Conceptual Design of Distributed Propellers Aircraft: Linear Aerodynamic Model Verification of Propeller-Wing Interaction in High-Lifting Configuration," *7 TH EUROPEAN CONFERENCE FOR AERONAUTICS AND AEROSPACE SCIENCES (EUCASS)*, 2017. https://doi.org/10.2514/6.2018-1742.

[17] Yoo, S., and Duensing, J., "Computational Analysis of the External Aerodynamics of the Unpowered X-57 Mod-III Aircraft," *AIAA Aviation 2019 Forum*, 2019. https://doi.org/10.2514/6.2019-3698, URL https://arc.aiaa.org/doi/abs/10.2514/6.2019-3698.

[18] Duensing, J., Housman, J., Maldonado, D., Jensen, J., Kiris, C., and Yoo, S., "Computational Simulations of Electric Propulsion Aircraft: the X-57 Maxwell," , 2019. URL https://www.nas.nasa.gov/pubs/ams/2019/06-13-19.html.

[19] Nguyen Van, E., Alazard, D., Pastor, P., and Döll, C., "Towards an Aircraft with Reduced Lateral Static Stability Using Differential Thrust," *2018 Aviation Technology, Integration, and Operations Conference*, 2018. https://doi.org/10.2514/6.2018-3209, URL https://arc.aiaa.org/doi/abs/10.2514/6.2018-3209.

[20] Nguyen Van, E., Alazard, D., Pastor, P., and Döll, C., "Co-design of aircraft vertical tail and control laws using distributed electric propulsion," *In IFAC Symposium on Automatic Control in Aerospace*, Cranfield, United Kingdom, Aug. 2018.

[21] Nguyen Van, E., "Lateral stability and control of an aircraft equipped with a small vertical tail by differential use of the propulsion systems. Use of co-design methods." Ph.D. thesis, ISAE-SUPAERO Institut Supérieur de l'Aéronautique et de l'Espace, Toulouse, France, Oct. 2020.

[22] Christophe, D., Delbecq, S., Defoort, S., Schmollgruber, P., Bernard, E., and Pommier-Budinger, V., "From FAST to FAST-OAD: An open source framework for rapid Overall Aircraft Design," *10th EASN International Conference*, Salerme, Italy, 2020. URL https://theses.hal.science/ONERA-MIP/hal-03182524v1.

[23] McDonald, R. A., and Gloudemans, J. R., "Open Vehicle Sketch Pad: An Open Source Parametric Geometry and Analysis Tool for Conceptual Aircraft Design," *AIAA SCITECH 2022 Forum*, January, 2022. https://doi.org/10.2514/6.2022-0004, URL https://arc.aiaa.org/doi/abs/10.2514/6.2022-0004.

[24] McCormick, B., *Aerodynamics of v/stol flight.*, Dover Publications, 1999.

[25] Drela, M., "XFOIL: An Analysis and Design System for Low Reynolds Number Airfoils," *Low Reynolds Number Aerodynamics*, edited by T. J. Mueller, Springer Berlin Heidelberg, Berlin, Heidelberg, 1989, pp. 1–12.

[26] Jameson, A., "Analysis of wing slipstream flow interaction," *NASA Contractor Reports*, 1970.

[27] Bouquet, T., and Vos, R., "Modeling the Propeller Slipstream Effect on Lift and Pitching Moment," *55th AIAA Aerospace Sciences Meeting*, 2017. https://doi.org/10.2514/6.2017-0236, URL https://arc.aiaa.org/doi/abs/10.2514/6.2017-0236.

[28] Planas, D., Pastor, P., and Döll, C., "Handling Qualities of a distributed propulsion electric aircraft," *In ICAS International Council of Aeronautical Sciences*, Stockholm, Sweden, 2022.

[29] "X-57 Maxwell," https://sacd.larc.nasa.gov/asab/asab-projects-2/x57maxwell/, 2023. Accessed: 2023-04-30.

[30] "X-57 Technical repository," https://www.nasa.gov/aeroresearch/X-57/technical/index.html, 2023. Accessed: 2023-4-30.

[31] "OpenVSP Hangar," https://hangar.openvsp.org/vspfiles/414, 2022. Accessed: 2022-11-30.

[32] Viken, J. K., Viken, S., Deere, K. A., and Carter, M., "Design of the Cruise and Flap Airfoil for the X-57 Maxwell Distributed Electric Propulsion Aircraft," *35th AIAA Applied Aerodynamics Conference*, 2017. https://doi.org/10.2514/6.2017-3922, URL https://arc.aiaa.org/doi/abs/10.2514/6.2017-3922.

[33] "JAVAFOIL," https://www.mh-aerotools.de/airfoils/javafoil.htm, 2018. Accessed: 2022-11-30.

[34] Litherland, B. L., Borer, N. K., and Zawodny, N. S., "X-57 Maxwell High-Lift Propeller Testing and Model Development," *AIAA AVIATION 2021 FORUM*, 2021. https://doi.org/10.2514/6.2021-3193, URL https://arc.aiaa.org/doi/abs/10.2514/6.2021-3193.

[35] Sachs, G., "Flight Performance Issues of Electric Aircraft." *AIAA Atmospheric Flight Mechanics Conference, No. 4727*, 2012.

[36] Deere, K., Viken, J., Viken, S., Carter, M., Wiese, M., and Farr, N., "Computational Analysis of a Wing Designed for the X-57 Distributed Electric Propulsion Aircraft," *AIAA Aviation 2017 Forum*, 2017, p. 3923. URL https://doi.org/10.2514/6.2017-3923.

[37] NASA, "Flight Demonstrations and Capabilities (FDC) Scalable Convergent Electric Propulsion Technology and Operations Research (SCEPTOR), Critical Design Review, Day 2 Package," 2016. URL https://doi.org/10.2514/6.2016-3920.